

High-Fidelity Lake Extraction via Two-Stage Prompt Enhancement: Establishing a Novel Baseline and Benchmark

Ben Chen^{1*}, Xuechao Zou^{1*}, Kai Li², Yu Zhang¹, Junliang Xing², Pin Tao^{1,2†}

¹Qinghai University, ²Tsinghua University

{benchen1997, xuechaozou}@163.com, tsinghua.kaili@gmail.com, tinkzy@163.com, {jlxing, taopin}@tsinghua.edu.cn

Abstract

The extraction of lakes from remote sensing images is a complex challenge due to the varied lake shapes and data noise. Current methods rely on multispectral image datasets, making it challenging to learn lake features accurately from pixel arrangements. This, in turn, affects model learning and the creation of accurate segmentation masks. This paper introduces a unified prompt-based dataset construction approach that provides approximate lake locations using point, box, and mask prompts. We also propose a two-stage prompt enhancement framework, LEPrompter, which involves prompt-based and prompt-free stages during training. The prompt-based stage employs a prompt encoder to extract prior information, integrating prompt tokens and image embeddings through self- and cross-attention in the prompt decoder. Prompts are deactivated once the model is trained to ensure independence during inference, enabling automated lake extraction. Evaluations on Surface Water and Qinghai-Tibet Plateau Lake datasets show consistent performance improvements compared to the previous state-of-the-art method. LEPrompter achieves mIoU scores of 91.48% and 97.43% on the respective datasets without introducing additional parameters or GFLOPs. Supplementary materials provide the source code, pre-trained models, and detailed user studies.

Introduction

Lakes are important environmental and climatic indicators and have received significant scientific attention (Lu et al. 2020). Global observation technology and sensing devices have made remote sensing imagery a popular tool for extracting water bodies (Wang, Gao, and Zhang 2021). Automated lake extraction from remote sensing imagery is crucial in monitoring climate change (Tian et al. 2023).

Lake extraction is primarily regarded as a semantic segmentation task for processing. Recently, researchers have employed deep learning techniques in the lake extraction task, such as UDGNet (Qin et al. 2020), to enhance the spatial resolution of lake regions. MSLWENet (Wang et al. 2020a) proposes an end-to-end multi-scale plateau lake extraction network model based on ResNet-101 (He et al. 2016) and depth-wise separable convolution (Chollet 2017). LEFormer (Chen et al. 2023a) utilizes a hybrid

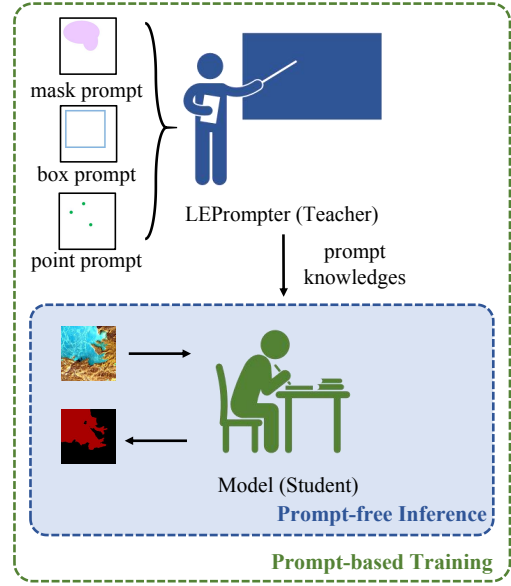


Figure 1: Our proposed two-stage prompt enhancement framework for lake extraction. The prompt-based approach simulates a teacher guiding students to solve challenging problems, while the prompt-free approach allows students to tackle problems independently. Conversely, the inference process exclusively utilizes the prompt-free approach.

CNN-Transformer architecture, HA-Net (Wang, Gao, and Zhang 2021) employs a mixed-scale attention model, and MSNANet (Lyu et al. 2022) adopts an encoder-decoder framework to enhance feature representation and achieve improved extraction results for lakes.

Existing lake datasets (Wang et al. 2020b) consist of multi-channel input images with single-channel ground truth, which poses challenges for model learning due to the complex pixel information and potential noise. The complexity of the pixel information requires models to capture intricate lake details effectively. Meanwhile, noise further hampers their performance, necessitating robust approaches to mitigate these issues and improve lake extraction accuracy. Moreover, these datasets exhibit high interclass heterogeneity and complex background information, including

*These authors contributed equally.

†Corresponding author.

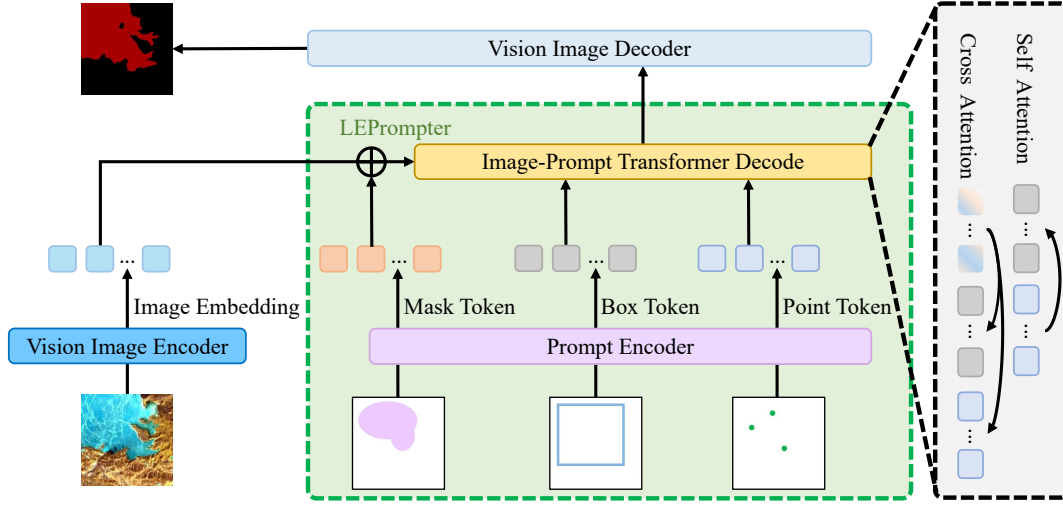


Figure 2: Overview architecture of LEPrompter with three main modules. (a) A prompt dataset that contains prior information. (b) A prompt encoder that extracts strong prior prompt information features. (c) A lightweight decoder that fuses the prompt tokens from the prompt encoder and the image embedding from the Vision Image Encoder to generate the final lake mask.

snow, glaciers, and mountains, introducing contextual ambiguity and additional challenges for accurate extraction.

Recently, prompt-based interactive semantic segmentation algorithms such as SAM (Kirillov et al. 2023) and SEEM (Zou et al. 2023) have shown promising performance by refining predicted masks through prompt prior information. However, these algorithms require a pre-prompt (point, box, or mask) alongside the input image, making them interactive. Additionally, SAM’s segmentation results lack semantic information, which restricts their suitability for fully automated interpretation of remote sensing images. Furthermore, both SAM and SEEM utilize extensive backbones (ViT-H (Dosovitskiy et al. 2020) and Focal-L (Yang et al. 2022)), leading to many model parameters and increased computational complexity during inference.

To address the limitations of existing datasets and models, we employ morphological operations to create a prompt dataset quickly. These datasets consist of point, box, and mask prompts based on the ground truth. We propose LEPrompter, a two-stage prompt enhancement framework for lake extraction from remote sensing imagery during training to effectively leverage the prompt dataset. The framework includes prompt-based and prompt-free stages. Training progresses in the prompt-based stage until reaching a specific step threshold. After that, we transition to the prompt-free stage, training the lake extraction model independently of prompts. In the prompt-based stage, the prompt dataset is processed by a lightweight prompt encoder and decoder, fused with the image embedding from the lake extraction model, generating output tokens for mask prediction. We use the prompt-free approach solely during inference. This approach requires no additional model parameters or GFLOPs during the inference process. The overall workflow is illustrated in Fig. 1, and the architecture of LEPrompter is shown in Fig. 2. The main contributions of our architecture

are summarized as follows:

- We develop a unified morphological method for generating various prompts and establish three types of prompt datasets (point, box, and mask) for lake extraction.
- We propose a two-stage prompt enhancement framework for automated lake extraction. This framework employs prompts to guide model training while allowing for independence from prompts during inference, serving as a baseline for lake extraction with prompt datasets.
- We evaluate the influence of prompt types for lake extraction and observe that a slight prompt positively guides model learning. Conversely, excessive prompts restrict performance improvement, aligning with the scenario of teachers guiding students in the real world.

Experimental results demonstrate that the prompt dataset and LEPrompter consistently improve the performance of the previous SOTA methods on the SW and QTPL datasets, achieving mIoU of 91.48% and 97.43%, respectively, without adding any parameters and GFLOPs. Compared to the previous SOTA method, LEFormer, applying the prompt dataset and LEPrompter, achieved the SOTA performance on the SW and QTPL datasets, respectively.

Based on the above main contributions and experimental results, the prompt dataset and the LEPrompter framework proposed in our study can serve as a benchmark and baseline for lake extraction tasks trained with prompts.

Related Work

Lake Extraction

Lake extraction aims to automatically locate the boundaries of a lake’s location from remote sensing imagery, and it belongs to the semantic segmentation task. Deep learning-based approaches for lake extraction have recently garnered

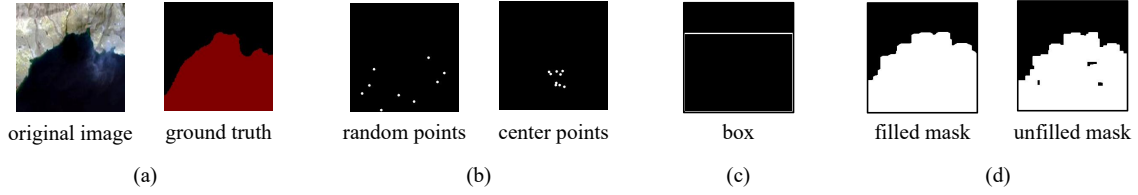


Figure 3: Visualization results of the prompt dataset for lake extraction. (a) Example images of the original image and ground truth. (b) Example images depicting two types of point prompts: random points and center points. (c) Example images illustrating box prompt. (d) Example images showcasing two types of mask prompts: filled mask and unfilled.

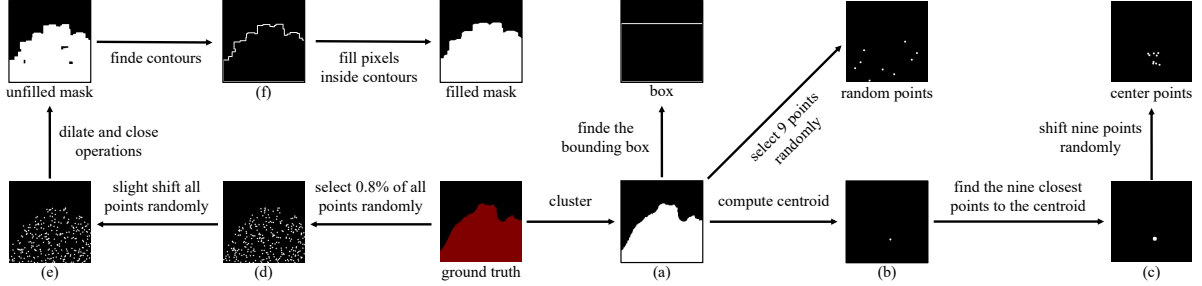


Figure 4: The workflow diagram of creating the prompt dataset for lake extraction.

significant attention from researchers. These approaches, such as UDGNet (Qin et al. 2020), aim to enhance the spatial resolution of lake regions. However, UDGNet needs help in effectively extracting features due to the diverse types and rich spatial-spectral characteristics of lakes, often resulting in the loss of crucial spatial information. To address these challenges, researchers explore integration strategies to optimize network structures and leverage multi-scale features specific to lake extraction. For instance, MSLWNet (Wang et al. 2020a) proposes an end-to-end multi-scale plateau lake extraction network model based on ResNet-101 (He et al. 2016) and depth-separable convolution (Chollet 2017). However, this model is susceptible to noise, particularly for lakes with intricate surface textures. Various approaches have been developed to overcome these challenges in the field of lake extraction. LEFormer (Chen et al. 2023a) utilizes a hybrid CNN-Transformer architecture, leveraging CNN to extract local features and the Transformer to capture global features. HA-Net (Wang, Gao, and Zhang 2021) employs a mixed-scale attention model, and MSNANet (Lyu et al. 2022) adopts an encoder-decoder framework to enhance feature representation and achieve improved extraction results for lakes. However, the extraction of lakes remains challenging due to high interclass heterogeneity and complex background information, such as snow, glaciers, and mountains, which introduce contextual ambiguity and pose additional extraction challenges.

Prompt Learning

Prompt learning is a technique that can help reduce semantic differences, bridge the gap between pre-training and fine-tuning, and prevent overfitting of the head. Since the introduction of GPT-3 (Brown et al. 2020), prompt learning has

advanced from traditional discrete and continuous prompt construction to large-scale model-oriented in-context learning (Alayrac et al. 2022), instruction-tuning (Liu et al. 2023), and chain-of-thought approaches (Wei et al. 2022). Current methods for constructing prompts mainly involve manual templates, heuristic-based templates, generation, word embedding fine-tuning, and pseudo tokens. Recently, prompt-based interactive semantic segmentation methods, such as SAM (Kirillov et al. 2023) and SEEM (Zou et al. 2023), have demonstrated remarkable performance in semantic segmentation. However, their applicability for fully automatic image segmentation is limited due to the requirement of pre-prompt input. Moreover, using extensive backbones in these algorithms, resulting in many model parameters and computational costs, poses a significant challenge. In the context of remote sensing images, APLeNet (Singha et al. 2023) and RSPrompter (Chen et al. 2023b) have successfully introduced the prompt mechanism and achieved good results. However, both methods necessitate additional model structures to extract prompt information during inference, resulting in increased parameters and computational costs.

The main aim of this study is to investigate the feasibility of using prompts in automatic lake extraction tasks rather than developing a universal zero-shot segmentation model. To this end, we generate images containing prompt information based on the ground truth, which assists in supervised training with the original dataset. However, during inference, we adopt a prompt-free approach, where the prompt information is no longer used, and only the original lake extraction model is employed to perform the task without any additional parameters or computational costs.

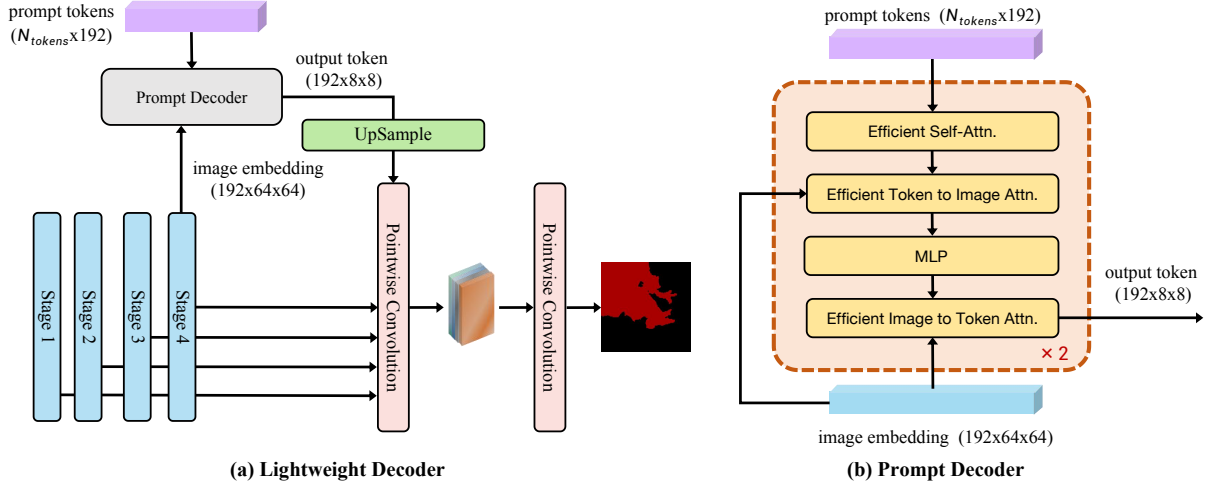


Figure 5: Overview architecture of lightweight decoder and prompt decoder.

Prompt-based Lake Extraction Dataset

In this work, we evaluated the accuracy and generalization capability of two publicly available satellite remote sensing datasets for lake extraction: the Surface Water dataset (SW dataset)¹ and the Qinghai-Tibet Plateau Lake dataset (QTPL dataset)² (Wang et al. 2020b). Both datasets include annotated lake water bodies and have a bit depth of 24 bits per pixel, including R, G, and B spectral bands. The SW dataset contains 17,596 images of size 256×256 , randomly divided into training and testing sets with a ratio of 4:1. In comparison, the QTPL dataset includes 6,773 images of size 256×256 , with a spatial resolution of 17 meters, randomly divided into training and testing sets with a ratio of 9:1. However, these datasets suffer from rich spatial-spectral characteristics of lakes, leading to the loss of crucial spatial information. Additionally, noise factors affect the model’s learning process. Moreover, these datasets present challenges of high interclass heterogeneity and complex background information, such as snow, glaciers, and mountains, introducing contextual ambiguity and additional extraction challenges.

Previous approaches have focused on improving the model for specific problems. In contrast, we directly improve the dataset to reduce the model’s learning difficulty. We employed the density-based clustering algorithm DBSCAN (Ester et al. 1996) and incorporated simple morphological operations, such as erosion and dilation, to refine the ground truth within the original dataset. This refinement process creates a specialized dataset called the prompt dataset. In contrast to interactive semantic segmentation models, such as SAM (Kirillov et al. 2023) and SEEM (Zou et al. 2023), our prompt dataset is generated directly from the ground truth by simulating human prompt habits, including point, box, and mask prompts, without relying on human interaction. The prompt dataset comprises five prompt types,

matching the number of images in the SW or QTPL datasets training set. No corresponding prompt dataset is available for the prompt-free testing set. For point prompts, we generate random and center points concentrated in the lake’s central area, with a maximum of nine points per type. Masks consist of filled masks with complete interiors and unfilled masks with partially unfilled interiors. The box prompt encompasses the entire lake. An example of the prompt data is shown in Fig. 3, and the workflow diagram for creating the prompt dataset is depicted in Fig. 4. The creation process for each prompt is summarized as follows:

- By applying DBSCAN clustering, we obtain the pixel map (a) of the lakes and randomly select nine points as prompts. We calculate the centroid of the pixels to generate an image (b) and identify the nine points closest to the centroid, resulting in the image (c). Finally, a slight shift is applied to the positions of these nine points to obtain the final center point prompt.
- We employ the pixel map (a) generated through DBSCAN clustering to ascertain the bounding box, consequently acquiring the box prompt.
- We randomly select 0.8% of the lake pixel points from the ground truth, resulting in an image (d). Applying a slight random shift produces an image (e). Next, we generate the unfilled mask prompt using dilate and close operations. To obtain the final filled mask prompt, we identify the contours of the unfilled mask, resulting in an image (f), and perform pixel-filling operations.

LEPrompter: Lake Extraction Prompter

In order to integrate the solid prior prompts from the prompt dataset into lake extraction models, we propose a two-stage prompt enhancement framework called LEPrompter. LEPrompter consists of two main modules:

- A prompt encoder that extracts solid prior prompt information features. Refer to the Prompt Encoder section for more details.

¹<https://aistudio.baidu.com/aistudio/datasetdetail/75148>

²<http://www.ncdc.ac.cn/portal/metadata/b4d9fb27-ec93-433d-893a-2689379a3fc0>

- A lightweight prompt decoder fuses the prompt tokens from the prompt encoder and the image embedding from the vision image encoder to generate the final lake mask. Refer to the Prompt Decoder section for more details.

LEPrompter is designed using a combination of prompt-based and prompt-free training during the training stage and prompt-free inference during the inference stage, as depicted in Fig. 1. The model can be considered a student in the training stage, while LEPrompter functions as a teacher. The teacher aids the student in solving challenging problems and provides correct answers. In contrast, the student receives guidance and trains in the right direction based on the correct prompts provided by LEPrompter. This helps prevent the model from getting stuck in locally optimal solutions.

Prompt Encoder

The primary function of the prompt encoder is to extract prompt tokens to assist in the training of the lake extraction model. The prompt encoder processes points and boxes to obtain sparse prompt embeddings (SPE), while masks are processed to obtain dense prompt embeddings (DPE). A point is represented as the sum of a positional encoding (Tancik et al. 2020) of its location and one of two learned embeddings indicating foreground or background. A box is represented by an embedding pair: the positional encoding of its top-left corner combined with a learned embedding for the "top-left corner" and a similar structure using a learned embedding indicating the "bottom-right corner." If there is no box prompt, the prompt encoder outputs a learned embedding representing "no box." The DPE has a spatial correspondence with the image embedding \mathbf{F} from VIE, achieved by downscaling them using a depth-wise separable convolution (Chollet 2017). Additionally, a GELU activation function (Hendrycks and Gimpel 2017) is applied, with the output channel dimension set to K . Similarly, if there is no mask prompt, the prompt encoder outputs a learned embedding representing "no mask." The prompt encoder can be expressed mathematically as:

$$\langle O_s, O_d \rangle = \text{PE}(Q; \langle P_p, P_b, P_m \rangle), \quad (1)$$

where Q is the learnable queries, and P_p, P_b, P_m represent the point, box, and mask prompts respectively. O_s and O_d represent to the SPE and DPE respectively. PE represents the prompt encoder.

Prompt Decoder

The prompt decoder is a lightweight decoder designed to calculate self- and cross-attention between the VIE's image embeddings and the prompt encoder's tokens. It then fuses the output with the vision image decoder (VID) to predict the mask. The prompt decoder is added to the VID at the position shown in Fig. 5(a). The image embedding \mathbf{F} is obtained by upsampling the feature map output by the last layer encoder of the VIE to a quarter of the original size and adding it element-wise with the DPE output by the prompt encoder. The resulting embedding has a size of $(K, 64, 64)$, while the prompt tokens from the SPE in the prompt encoder have a size of $(N_{tokens} \times K)$, where the specific value of

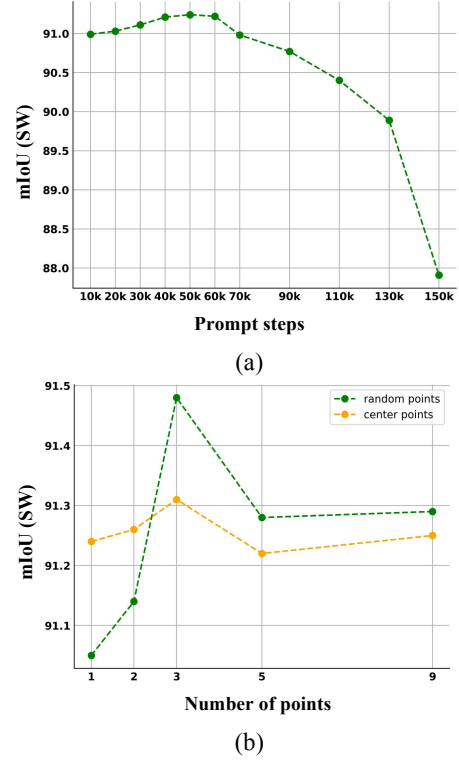


Figure 6: Quantitative analysis of ablation studies. (a) Influence of the prompt-based steps. (b) Influence of the type and number of prompt points on the lake extraction task.

N_{tokens} is determined by the positions of the two points encoding the points and boxes. Our prompt decoder design, shown in Fig. 5(b), consists of two Image-Prompt Transformer Blocks (IPTB). Each IPTB performs four steps:

- Efficient self-attention on the tokens.
- Efficient cross-attention from tokens (as queries) to the image embedding.
- A point-wise MLP updates each token
- Efficient cross-attention from the image embedding (as queries) to tokens.

This last step updates the image embedding with prompt information. To reduce the complexity of the self- and cross-attention mechanism, we use the PVT (Wang et al. 2021). Each self- and cross-attention and MLP has a residual connection (He et al. 2016) and a layer normalization.

$$O_d = \text{Conv}(\mathbf{F} + O_d), \quad (2)$$

$$\langle O_d, O_s \rangle = \text{IPTB}(O_d, O_s). \quad (3)$$

The next IPTB takes the updated SPE O_s and the updated DPE O_d from the previous layer and outputs an output token of size $(K, 8, 8)$. The output token is then upsampled to a quarter of the original size and concatenated with other image embeddings from the VIE. Finally, the concatenated embeddings are fed to the VID for mask prediction.

Point		Box	Mask		SW		
CP	RP		FK	UFK	OA↑	F1↑	mIoU↑
					95.63	95.19	90.86
✓					95.86	95.44	91.31
	✓				95.95	95.53	91.48
		✓			95.79	95.36	91.17
			✓		95.77	95.34	91.14
				✓	95.77	95.34	91.13
✓		✓			95.77	95.34	91.12
	✓	✓			95.76	95.33	91.11
✓			✓		95.65	95.21	90.89
✓				✓	95.67	95.23	90.93
	✓		✓		95.66	95.22	90.90
	✓			✓	95.66	95.22	90.91
		✓	✓		95.66	95.22	90.91
		✓		✓	95.67	95.23	90.94
✓		✓	✓		95.64	95.20	90.88
✓		✓		✓	95.63	95.19	90.85
	✓	✓	✓		95.66	95.22	90.91
	✓	✓		✓	95.66	95.21	90.90

Table 1: Ablation studies on the different combinations of prompts. CP, RP, FK, and UFK represent center points, random points, filled masks, and unfilled masks, respectively.

Experiments

Experimental Settings

Implementation Details. In this study, we trained all models on a single Tesla V100 GPU using the *MMSegmentation* (Contributors 2020) codebase for 160K iterations on the SW with SW prompt and QTPL with QTPL prompt datasets. We applied data augmentation techniques, such as random resizing and horizontal flipping, to avoid overfitting and improve generalization. We used the AdamW (Loshchilov and Hutter 2018) optimizer and the cross-entropy loss function with a batch size of 16. The initial values of the learning rate and weight decay were set to 6×10^{-5} and 0.01, respectively. A PolyScheduler (He et al. 2017) with a default factor of 1.0 was then used to adjust the learning rate dynamically.

Evaluation Metrics. We conducted a user study to compare with four baseline lake extraction methods (Xie et al. 2021; Yu et al. 2022; Guo et al. 2022; Chen et al. 2023a). During the study, participants were presented with the ground truth image and two predicted masks: one generated by the original model and the other enhanced with prompt dataset and LEPrompter. Their task was to select the image that closely resembled the ground truth. To ensure impartiality, the methods were anonymized and randomly presented for each image. The user study evaluated 200 randomly selected images, comprising 100 images from the SW dataset and 100 from the QTPL dataset. Each image received responses from 15 participants, resulting in 3000 votes. This process was repeated ten times, and the final outcome was determined by computing the mean votes across the ten iterations. Additionally, we assessed the models’ accuracy using metrics such as overall accuracy (OA), F1-Score, and mean Intersec-

tion over Union (mIoU).

Ablation Studies

Compared to QTPL, the SW dataset presents more significant challenges due to its higher pixel complexity and a higher presence of interclass heterogeneity and complex background information, such as snow, glaciers, and mountains. Therefore, we selected the SW dataset to evaluate our proposed ablation study method. To more rigorously evaluate our proposed method’s effectiveness, we conducted additional ablation studies on the SW with the prompt dataset using LEPrompter with LEPrompter.

Influence of the prompt-based steps of the model. We first analyze the impact of increasing the number of prompt-based training steps with LEPrompter. Fig. 6 (a) illustrates that as the number of prompt-based training steps increases, the model’s mIoU gradually improves, reaching a peak of 91.48% at 50k steps. However, since LEPrompter is only used during the training phase, and the inference phase is prompt-free, an excessive number of prompt-based training steps may cause the model to overly rely on LEPrompter’s assistance, resulting in inadequate independent fitting of the dataset and a decrease in mIoU. Therefore, as the number of steps exceeds 50k, the model’s mIoU gradually decreases or may even fall below the mIoU achieved by the model without LEPrompter. Overall, using LEPrompter appropriately has a significant positive impact on the model’s accuracy. We have identified 50k steps as the most suitable number of prompt-based training steps, and all subsequent experiments are performed using this value.

Influence of the type and number of prompt points. We are currently analyzing the influence of the type and number of prompt points. Ablation experiments are being conducted to evaluate the impact of two types of prompt points (center points vs random points) and the number of prompt points ranging from 1 to 9 for each type. The experimental results are illustrated in Fig. 6 (b). Regardless of whether center points or random points are used, the mIoU of LEPrompter increases as the number of selected points increases, reaching its maximum value when the number of points is 3, followed by a slight decrease. Initially, the accuracy of the random points method is lower than that of the center points method when the number of points is 1 or 2. However, it gradually overtakes center points as the number of points increases and maintains a leading position. This could be explained by the fact that when the number of points is small, the random points method tends to select points located in the edge areas of the lake, while center points are concentrated in the lake’s central region. As a result, the center points provide relatively more information about the selected points. As the number of points increases, the random points method can better reflect the approximate shape of the lake. In contrast, the center points method is concentrated in one area, which cannot reflect the approximate shape of the lake when the lake area is relatively large. We selected 3 random points in all subsequent experiments involving prompt points.

Influence of the combination of prompts. In this experiment, we investigate the impact of different prompt combinations on improving model accuracy and identify the most

Method	SW				QTPL			
	OA \uparrow	F1-Score \uparrow	mIoU \uparrow	Vote [%]	OA \uparrow	F1-Score \uparrow	mIoU \uparrow	Vote [%]
SegFormer	95.58	93.65	90.75	10.93	98.66	98.62	97.27	20.00
SegFormer*	95.91(+0.33)	95.49(+0.36)	91.40(+0.65)	89.07	98.69(+0.03)	98.64(+0.02)	97.33(+0.06)	80.00
PoolFormer	94.65	94.09	88.90	9.07	98.59	98.54	97.13	14.40
PoolFormer*	95.12(+0.47)	94.62(+0.53)	89.84(+0.94)	90.93	98.62(+0.03)	98.58(+0.04)	97.20(+0.07)	85.60
SegNeXt	95.50	95.05	90.61	10.40	98.60	98.55	97.15	9.07
SegNeXt*	95.59(+0.09)	95.14(+0.09)	90.77(+0.16)	89.60	98.65(+0.05)	98.60(+0.05)	97.24(+0.09)	90.93
LEFormer	95.63	95.19	90.86	12.53	98.74	98.69	97.42	15.47
LEFormer*	95.95(+0.32)	95.53(+0.34)	91.48(+0.62)	87.47	98.74(-)	98.70(+0.01)	97.43(+0.01)	84.53

Table 2: Quantitative comparison of four methods with and without our proposed prompt dataset and LEPrompter on the SW and QTPL datasets. The asterisk (*) denotes the utilization of prompt dataset and LEPrompter.

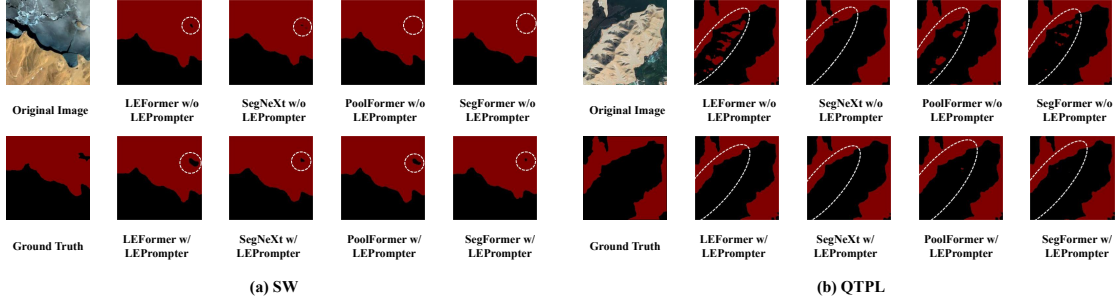


Figure 7: Visualization results of four methods without our proposed prompt dataset and LEPrompter, and with prompt dataset and LEPrompter, on the SW and QTPL datasets for lake mask extraction. The white circles highlight noticeable differences.

effective combination. To achieve this, we conducted experiments on the SW prompt dataset, using five distinct prompts with 17 prompt combinations. Table 1 shows the accuracy of each combination. Our results indicate that the majority of prompt combinations have a positive effect on the accuracy of the LEFormer. Only a few combinations have slightly lower accuracy than the baseline. The effectiveness of the prompts gradually diminishes as the number of prompts increases. This finding is consistent with the above observation, where an increase in the number of points results in a decrease in the improvement of model accuracy. Based on these results, we can conclude that our proposed prompt dataset and LEPrompter significantly improve the model’s accuracy. However, if too many prompts are used, the effectiveness of this improvement will gradually diminish. We selected only three random points as the optimal combination of prompts and conducted subsequent experiments.

Comparison with State-of-the-Art Methods

We evaluated the prompt dataset and LEPrompter by comparing them with advanced lake extraction models (Xie et al. 2021; Yu et al. 2022; Guo et al. 2022) on the SW and QTPL datasets. Table 2 shows the quantitative results, including the OA, F1-Score, mIoU and the votes from the user study. In addition, Fig. 7 shows the visualization results.

The results presented in Table 2 demonstrate the significant accuracy improvement achieved by the prompt dataset with LEPrompter on both benchmark datasets. Applying the prompt dataset with the LEPrompter framework to LEFormer resulted in mIoU values of 91.48% and 97.43%

on the SW and QTPL datasets, respectively. This represents a 0.62% and 0.01% improvement over the previous SOTA methods. The user study showed that the model enhanced with prompt dataset and LEPrompter received over 80% of the votes, indicating that the generated masks closely resemble the ground truth. Moreover, the prompt-free stage of LEPrompter enables improved accuracy without any additional parameters or GFLOPs, avoiding hardware cost increases. In summary, the results demonstrate that the prompt dataset with LEPrompter is a superior auxiliary framework for lake extraction tasks regarding the accuracy, computation cost, and model size.

Conclusion

In this work, we present three types of prompt datasets (point, box, and mask) for lake extraction and a two-stage prompt enhancement framework called LEPrompter. Prompt datasets and LEPrompter aim to improve the accuracy of lake extraction methods without increasing the model’s learning difficulty or incorporating excessive noise information. The prompt datasets were created by applying morphological operations to the ground truth in the original dataset. The LEPrompter can be easily integrated into existing lake extraction methods to improve accuracy. During inference, pre-trained models can be directly loaded without any modification. Experimental results demonstrate that the prompt datasets and LEPrompter significantly enhance the accuracy of automated lake extraction on two popular datasets. We believe that this study will facilitate the research of lake extraction tasks and inspire further research in this domain.

References

- Alayrac, J.-B.; Donahue, J.; Luc, P.; Miech, A.; Barr, I.; Hasson, Y.; Lenc, K.; Mensch, A.; Millican, K.; Reynolds, M.; et al. 2022. Flamingo: a visual language model for few-shot learning. *NeurIPS*, 35: 23716–23736.
- Brown, T.; Mann, B.; Ryder, N.; Subbiah, M.; Kaplan, J. D.; Dhariwal, P.; Neelakantan, A.; Shyam, P.; Sastry, G.; Askell, A.; et al. 2020. Language models are few-shot learners. *NeurIPS*, 33: 1877–1901.
- Chen, B.; Zou, X.; Zhang, Y.; Li, J.; Li, K.; and Tao, P. 2023a. LEFormer: A Hybrid CNN-Transformer Architecture for Accurate Lake Extraction from Remote Sensing Imagery. arXiv:2308.04397.
- Chen, K.; Liu, C.; Chen, H.; Zhang, H.; Li, W.; Zou, Z.; and Shi, Z. 2023b. RSPrompter: Learning to Prompt for Remote Sensing Instance Segmentation based on Visual Foundation Model. arXiv:2306.16269.
- Chollet, F. 2017. Xception: Deep learning with depthwise separable convolutions. In *CVPR*, 1251–1258.
- Contributors, M. 2020. MMSegmentation: OpenMMLab Semantic Segmentation Toolbox and Benchmark. <https://github.com/open-mmlab/mms Segmentation>.
- Dosovitskiy, A.; Beyer, L.; Kolesnikov, A.; Weissenborn, D.; Zhai, X.; Unterthiner, T.; Dehghani, M.; Minderer, M.; Heigold, G.; Gelly, S.; et al. 2020. An Image is Worth 16x16 Words: Transformers for Image Recognition at Scale. In *ICLR*.
- Ester, M.; Kriegel, H.-P.; Sander, J.; Xu, X.; et al. 1996. A density-based algorithm for discovering clusters in large spatial databases with noise. In *KDD*, 34, 226–231.
- Guo, M.-H.; Lu, C.-Z.; Hou, Q.; Liu, Z.; Cheng, M.-M.; and Hu, S.-M. 2022. Segnext: Rethinking convolutional attention design for semantic segmentation. *NeurIPS*, 35: 1140–1156.
- He, K.; Gkioxari, G.; Dollár, P.; and Girshick, R. B. 2017. Mask R-CNN. *ICCV*, 2980–2988.
- He, K.; Zhang, X.; Ren, S.; and Sun, J. 2016. Deep residual learning for image recognition. In *CVPR*, 770–778.
- Hendrycks, D.; and Gimpel, K. 2017. Bridging Nonlinearities and Stochastic Regularizers with Gaussian Error Linear Units. In *ICLR*.
- Kirillov, A.; Mintun, E.; Ravi, N.; Mao, H.; Rolland, C.; Gustafson, L.; Xiao, T.; Whitehead, S.; Berg, A. C.; Lo, W.-Y.; Dollár, P.; and Girshick, R. 2023. Segment Anything. arXiv:2304.02643.
- Liu, H.; Li, C.; Wu, Q.; and Lee, Y. J. 2023. Visual Instruction Tuning. *CoRR*, abs/2304.08485.
- Loshchilov, I.; and Hutter, F. 2018. Decoupled Weight Decay Regularization. In *ICLR*.
- Lu, J.; Qiu, Y.; Wang, X.; Liang, W.; Xie, P.; Shi, L.; Menenti, M.; and Zhang, D. 2020. Constructing dataset of classified drainage areas based on surface water-supply patterns in High Mountain Asia. *BIG EARTH DATA*, 4(3): 225–241.
- Lyu, X.; Fang, Y.; Tong, B.; Li, X.; and Zeng, T. 2022. Multi-scale Normalization Attention Network for Water Body Extraction from REMOTE SENS-BASEL Imagery. *REMOTE SENS-BASEL*, 14(19): 4983.
- Qin, M.; Hu, L.; Du, Z.; Gao, Y.; Qin, L.; Zhang, F.; and Liu, R. 2020. Achieving higher resolution lake area from REMOTE SENS-BASEL images through an unsupervised deep learning super-resolution method. *REMOTE SENS-BASEL*, 12(12): 1937.
- Singha, M.; Jha, A.; Solanki, B.; Bose, S.; and Banerjee, B. 2023. APPLeNet: Visual Attention Parameterized Prompt Learning for Few-Shot REMOTE SENS-BASEL Image Generalization using CLIP. In *CVPR*.
- Tancik, M.; Srinivasan, P.; Mildenhall, B.; Fridovich-Keil, S.; Raghavan, N.; Singhal, U.; Ramamoorthi, R.; Barron, J.; and Ng, R. 2020. Fourier features let networks learn high frequency functions in low dimensional domains. *NeurIPS*, 33: 7537–7547.
- Tian, Z.; Guo, X.; He, X.; Li, P.; Cheng, X.; and Zhou, G. 2023. MSCANet: multiscale context information aggregation network for Tibetan Plateau lake extraction from REMOTE SENS-BASEL images. *IJDE*, 16(1): 1–30.
- Wang, W.; Xie, E.; Li, X.; Fan, D.-P.; Song, K.; Liang, D.; Lu, T.; Luo, P.; and Shao, L. 2021. Pyramid vision transformer: A versatile backbone for dense prediction without convolutions. In *ICCV*, 568–578.
- Wang, Z.; Gao, X.; and Zhang, Y. 2021. HA-Net: A lake water body extraction network based on hybrid-scale attention and transfer learning. *REMOTE SENS-BASEL*, 13(20): 4121.
- Wang, Z.; Gao, X.; Zhang, Y.; and Zhao, G. 2020a. MSLWENet: A novel deep learning network for lake water body extraction of Google REMOTE SENS-BASEL images. *REMOTE SENS-BASEL*, 12(24): 4140.
- Wang, Z.; Gao, X.; Zhang, Y.; and Zhao, G. 2020b. MSLWENet: A novel deep learning network for lake water body extraction of Google REMOTE SENS-BASEL images. *REMOTE SENS-BASEL*, 12(24): 4140.
- Wei, J.; Wang, X.; Schuurmans, D.; Bosma, M.; Xia, F.; Chi, E.; Le, Q. V.; Zhou, D.; et al. 2022. Chain-of-thought prompting elicits reasoning in large language models. *NeurIPS*, 35: 24824–24837.
- Xie, E.; Wang, W.; Yu, Z.; Anandkumar, A.; Alvarez, J. M.; and Luo, P. 2021. SegFormer: Simple and efficient design for semantic segmentation with transformers. *NeurIPS*, 34: 12077–12090.
- Yang, J.; Li, C.; Dai, X.; and Gao, J. 2022. Focal modulation networks. *NeurIPS*, 35: 4203–4217.
- Yu, W.; Luo, M.; Zhou, P.; Si, C.; Zhou, Y.; Wang, X.; Feng, J.; and Yan, S. 2022. Metaformer is actually what you need for vision. In *CVPR*, 10819–10829.
- Zou, X.; Yang, J.; Zhang, H.; Li, F.; Li, L.; Wang, J.; Wang, L.; Gao, J.; and Lee, Y. J. 2023. Segment Everything Everywhere All at Once. arXiv:2304.06718.